Flow behaviour of entangled surfactant micelles



1996 J. Phys.: Condens. Matter 8 9167

(http://iopscience.iop.org/0953-8984/8/47/006)

J. Phys.: Condens. Matter **8** (1996) 9167–9176. Printed in the UK

# Flow behaviour of entangled surfactant micelles

M E Cates

Department of Physics and Astronomy, University of Edinburgh, JCMB, King's Buildings Mayfield Road, Edinburgh EH9 3JZ, UK

Received 24 July 1996

**Abstract.** Many viscoelastic surfactant solutions contain giant, self-assembled micelles. These can be described as 'living polymers', whose chains are subject to reversible scission and recombination. Their dynamics in the entangled regime is accordingly modified from the reptation picture for conventional polymer chains. For rapid scission kinetics, the linear viscoelastic spectrum approaches a single-exponential (Maxwell) behaviour: small departures from this can be measured, and the model used to deduce information both on the micellar kinetics (the lifetime of a typical micelle before breaking) and on the structure (the mean micelle length). These ideas work for several systems, but for others, unreasonable trends for these quantities are found. The most likely reason for this is micellar branching effects, which (as far as the reptation–reaction model is concerned) introduce an effective micellar length equal to the mean distance between branch points. Another possible discrepancy comes from the breakdown of mean-field averaging for the micellar reactions. The reptation–reaction model yields a non-linear constitutive equation which shows a non-monotonic dependence of stress on strain rate, in simple steady shear. This leads one to expect flow instabilities, and (with further assumptions) suggests that steady shear-banded flows should arise, in which macroscopic layers of fluid of different shear rates coexist. Several experimental observations support this general picture, although the same instability could instead lead to wall slip, or unsteady flows.

## 1. Introduction

Surfactant molecules in solution have a strong tendency to aggregate reversibly into extended structures. Depending on the local molecular geometry, the basic packing unit can range from a small sphere (conventional micelles), through long, sometimes flexible cylinders (giant micelles), on to bilayers (e.g. smectic phases). For a recent review, see [1]. The parameters controlling this sequence mainly involve the relative sizes of the polar head group and the hydrophobic tail [2]. In what follows, we assume the preferred packing geometry to be a semiflexible cylinder and discuss the dynamics of the resulting giant micelles. Like most isotropic phases of surfactants, these are in full thermodynamic equilibrium.

Giant micelles can be viewed as one of a larger group of systems: 'living polymers' which are reversibly polymerizing chain-like objects that arise in equilibrium through self-assembly of smaller units. In the case of giant micelles, the diameter of our 'polymer' is of order 3 nm and a typical persistence length is 15 nm. The contour length $L$ is variable, governed by thermodynamic equilibrium, and in some systems extremely large (up to about 1 mm). For reviews, see [3–6], which contain many important references omitted below.

We suppose the number per unit volume of chains of arc-length $L$ to be $c(L)$, and choose units so that the 'volume fraction' is the same as the arc-length density:

$$\phi = \int_0^\infty Lc(L)\ \mathrm{d}L. \tag{1}$$

0953-8984/96/479167+10$19.50  

Then the gaussian size of a chain (which is a random walk) is given by $L^{1/2}$, with a prefactor (which we ignore) dependent on the local chain geometry. The packing energy of a chain can be written as $AL + E$, where the term linear in $L$ comes from the body of the chain and the constant term $E$ is that required to create two chain ends (i.e., hemispherical end-caps in the case of micelles). This is typically 5–25 kT. We have in the Flory–Huggins approach the following free-energy density [7]:

$$F = \int_0^\infty c(L)\,[kT\ \ln c(L) + E + AL] + F_{int}(\phi). \tag{2}$$

Here the final term arises from interactions between micelles. Insofar as this depends only on the total concentration $\phi$ it has no impact on the size distribution and may be dropped. Minimizing $F$ at fixed $\phi$ gives the size distribution

$$c(L) \simeq \mathrm{e}^{-E/kT}\mathrm{e}^{-L/\bar{L}} \tag{3}$$

where $\bar{L} = \phi^{1/2}\mathrm{e}^{E/2kT}$. Thus we have a broad distribution of chain lengths with a mean that increases slowly with $\phi$, and rapidly with $E$. Slightly different results are obtained if excluded-volume correlations are included [8].

## 2. Kinetics of micelles

In a system of living polymers, the chains can break and recombine reversibly. Various mechanisms are possible.

(i) Reversible scission: a chain breaks randomly anywhere along its length. The reverse reaction is end-to-end fusion.

(ii) End interchange: the end of one chain attacks the central part of another. The reverse reaction is the same process.

(iii) Bond interchange: two chains swap a central bond via a four-armed intermediate. The reverse reaction is the same process.

Other mechanisms, such as the shedding of individual surfactant molecules from a micelle (leading to infinitesimal length changes) are important for small micelles but not giant ones—because their effect on the size of a large object is very small compared to that of the processes listed above.

The kinetics can be probed experimentally by the temperature-jump method [9, 10]. If the temperature is suddenly changed (e.g. by a capacitor discharge), $\bar{L}$ is altered and $c(L)$ must relax to the new distribution. The relaxation is probed by light scattering which is (weakly) sensitive to the size distribution. Expanding perturbatively for a small jump $\epsilon$ gives $\Delta c(L, t = 0) = \epsilon\,(L - \bar{L})\exp[-L/\bar{L}]$. To calculate the time evolution one must substitute this into suitable kinetic equations describing the mechanisms (i)–(iii) above. For example in reversible scission one has the mean-field kinetic equation for the size distribution

$$\dot{c}(L) = -k_1 L c(L) + 2k_1 \int_L^\infty c(L')\ \mathrm{d}L' + \frac{1}{2}k_2 \int_0^\infty c(L')c(L - L')\ \mathrm{d}L' - k_2 \int_0^\infty c(L')\ \mathrm{d}L'.$$

The first term represents scission of chains of length $L$, the second scission of chains of length $L' > L$ (to give a chain of length $L$), the third is the combination of two smaller chains to make one of length $L$, and the fourth term represents loss of chains of length $L$ by combination with another chain. The rate constants must obey $k_1/k_2 = \mathrm{e}^{-E/kT}$, imposed by demanding that the steady-state solution corresponds to the thermodynamic equilibrium distribution. Linearizing the above kinetic equation and solving with the appropriate initial

condition gives an exponential decay with rate constant $2/\tau_b$ [10]. Here $\tau_b = 1/k_1\bar{L}$ is the waiting time for a break on a chain of the mean length. End interchange and bond interchange have similar kinetic equations. However, in both cases, the $T$-jump corresponds to a 'zero mode': the perturbation $\Delta c(L, 0)$ does not decay in time [11, 12]. The presence of a zero mode is linked in each case to the fact that the reaction scheme preserves the total number of chains in the system. This means that in these systems, the $T$-jump experiment does not measure the mean breaking time, although this remains the most important kinetic parameter.

The main problem with the $T$-jump method is that the relevant signal (usually a change in the static light scattering) becomes very small in the entangled regime. Such scattering measurements, for the same reason, cannot be used directly to detect $\bar{L}$. Clearly, some other method is needed to get unambiguous structural and kinetic information for micelles in the entangled regime. It turns out that the study of small-amplitude flow behaviour is well adapted to this role.

The kinetic scheme written above for reversible scission, and similar ones that we have studied for the interchange processes [11, 12], are based on simple mean-field assumptions. In essence, we assume that a given chain end, formed in (say) a scission reaction, is more likely to recombine in due course with an end of an independent chain, than with the very same end that it split away from in the original scission event. This can break down under certain conditions [13], discussed further below.

## 3. Polymer dynamics

The dynamics of unbreakable chains is nowadays understood in terms of the tube model. This describes motion at scales larger than the tube diameter $a \sim L_e^{1/2}$ where $L_e$ is the 'entanglement length' (the contour length of a marginally entangled chain). To model the entangled state, each chain is imagined confined to a tube of radius $a$ [14]. The tube has $N_T = L/L_e$ 'tube segments', arranged in a random walk, each having $\Delta s \simeq L_e$ monomers. The chain can diffuse only along the axis of the tube by 'reptation'; as it emerges, a new tube is created. There is a curvilinear diffusion constant $D_c(L) \sim 1/L$, this proportionality arising because the frictional drag on a chain is proportional to its length. The chain conformation is fully relaxed on the time-scale for complete escape from the tube. This requires curvilinear diffusion over a length $L$, and hence the relaxation time scales as $\tau_{rep} \sim L^3$. Typical reptation times for long, unbreakable chains are 0.1 s–1 h.

We consider a set of chains in a volume $V$ and coarse-grain into subunits $i$ of length $\Delta s = L_e$, each with an end-to-end vector $\Delta \boldsymbol{r}_i$. Each contributes $(p_i)_\beta (f_i)_\alpha$ to the elastic stress tensor $\sigma_{\alpha\beta}$ in our material, where $\alpha, \beta$ are cartesian indices. The quantity $(p)_\beta = \Delta r_\beta / V$ is the probability per unit area that a subunit crosses a given plane perpendicular to $\beta$, whereas $f_\alpha = kT\,\Delta r_\alpha / \Delta s$ is the thermodynamic force (spring tension) in the subunit. Hence the total contribution is

$$\sigma_{\alpha\beta}^{pol} = \frac{kT}{V} \sum_i \frac{\Delta r_\beta\, \Delta r_\alpha}{\Delta s}. \tag{4}$$

In practice, the stress tensor also has contributions from the isotropic pressure $P$ and from velocity gradients in the solvent: $\sigma_{\alpha\beta} = \sigma_{\alpha\beta}^{pol} + \sigma_{\alpha\beta}^{sol} + P\delta_{\alpha\beta}$.

The simplest rheological measurements involve the linear viscoelastic response of a material to small deformations. Consider, for example, an imposed strain, $x \to x + \gamma y$, with $\gamma$ the strain angle (assumed small) suddenly imposed at time zero and then held

constant. The response is

$$\sigma_{xy}(t) = \gamma G(t) \tag{5}$$

where we can write $G(t) = G_0\mu(t)$ as the product of an instantaneous shear modulus (the plateau modulus) and a memory function $\mu(t)$. In a polymeric system, the stress will not fully decay until chains have had time to relax their contribution to the stress tensor by adapting their configurations to the strained shape of the sample. A related experiment examines oscillatory shear, $\gamma = \gamma_0 e^{i\omega t}$, for which the stress is

$$\sigma_{xy}(t) = G^*(\omega)\gamma \tag{6}$$

with $G^*(\omega) = G'(\omega) + iG''(\omega)$ where $G', G''$ are called the storage modulus and the loss modulus. Linear response theory shows that

$$G^*(\omega) = i\omega \int_0^\infty G(t)e^{-i\omega t}\, dt. \tag{7}$$

An example is the Maxwell fluid, $\mu(t) = e^{-t/\tau}$ which has

$$G'(\omega) = \frac{G_0\omega^2\tau^2}{1+\omega^2\tau^2} \qquad G''(\omega) = \frac{G_0\omega\tau}{1+\omega^2\tau^2}. \tag{8}$$

When plotted in the 'Cole–Cole' representation (a plot of $G''$ versus $G'$ with frequency parametrically eliminated) this gives a perfect semicircle. Remarkably, many entangled micellar systems approximate very closely the idealized Maxwell response. This is not true for normal polymeric samples (especially with a spread of chain lengths present).

Under most conditions [14] the stress formula (4) for gaussian chains can be written as

$$\sigma_{\alpha\beta}^{pol} = (\phi/L_e)\, kT\, W_{\alpha\beta} \tag{9}$$

where $W_{\alpha\beta} = \langle u_\alpha u_\beta \rangle$ (the average is over tube segments, and $\boldsymbol{u}$ is a unit tangent to the tube). In an undeformed state, $W_{\alpha\beta} = \delta_{\alpha\beta}/3$ which contributes an irrelevant pressure term. If a step strain $\gamma$ is now applied, we have the instantaneous deformation $\boldsymbol{u} \to \boldsymbol{u} + \delta\boldsymbol{u}$ where $\delta\boldsymbol{u} = (\gamma u_y, 0, 0)$. A simple calculation then shows

$$\sigma_{xy}(t = 0^+) = G_0\gamma \tag{10}$$

where $G_0 = (4/15)(\phi/L_e)kT$ is the plateau modulus. In practice, this serves as an operational definition of the entanglement length.

As time proceeds, each chain escapes by curvilinear diffusion from its tube. A new tube is created as the chain moves, but this is in isotropic equilibrium in the strained environment. Hence $\mu(t)$ is the fraction of the $t = 0$ tube through which neither chain end has passed, up to time $t$. This is found by imagining the tube diffusing relative to a fixed chain, and studying the survival probability of a labelled tube segment. This 'particle' diffuses at a rate $D_c$ and is killed when it meets either end of the chain on which it resides. The result is a fairly monoexponential relaxation [14]. However, if one has a distribution of chain lengths, the relaxation spectrum can be estimated (at the crudest level) by taking the weighted average

$$\bar{\mu}(t) \simeq \int Lc(L)\, \mu_L(t)\, dL \Big/ \int Lc(L)\, dL. \tag{11}$$

For micellar systems, with an exponential size distribution, this would predict an extremely non-exponential decay. A variety of more sophisticated estimates lead to the same basic conclusion.

## 4. Linear viscoelasticity of giant micelles

On instantaneous deformation, living polymers behave just as 'dead' ones do, and the plateau modulus is $G_0 = (4/15)\phi/L_e$ as before. To describe the subsequent relaxation, we now have two time-scales: $\tau_b$ and $\tau_{rep}$ characterizing micellar reactions and diffusion respectively. When $\tau_b \gg \tau_{rep}$ there is no direct effect of breaking reactions and a formula like (11) can be used. This gives $\mu(t) \sim \exp[-(t/\tau_{rep}(\bar{L}))^{1/4}]$. This sort of decay has been reported in certain systems [15]. More commonly, however, entangled micelles approach the ideal limit of the Maxwell fluid: $\mu(t) \sim \mathrm{e}^{-t/\tau}$. This in fact corresponds to the fast-breaking limit, $\tau_b \ll \tau_{rep}$.

In this limit, the relaxation function $\mu(t)$ can be calculated numerically from a one-dimensional stochastic model in which a randomly chosen tube segment diffuses relative to a chain. As in the unbreakable-chain calculation, the particle is absorbed upon reaching a chain end and $\mu(t)$ is its survival probability. The chain length is now a function of time, however, and the chain ends make discrete jumps corresponding to reactions in which parts of the chain are removed and other parts added. The rate constants for these processes can be determined from the kinetic equations according to any of the three schemes discussed above. For $\tau_b \ll \tau_{rep}$, a monoexponential relaxation is indeed approached with a relaxation time $\tau$ that varies as $(\tau_b\tau_{rep})^{1/2}$ for reversible scission and end interchange, but as $\tau_b^{1/3}\tau_{rep}^{2/3}$ for bond interchange [16, 11, 12]. The physical origin of monoexponential behaviour is a separation of time-scales: the stress relaxation time $\tau$ remains large compared to $\tau_b$ when $\tau_b \ll \tau_{rep}$. Many reactions occur on a given chain before a typical tube segment is relaxed; this gives a fast averaging effect on the time-scale $\tau_b$ within which the various tube segments become mixed up with one another. Correspondingly, each sees an average decay and all tube segments relax with the same rate.

Corrections to the monoexponential behaviour can be computed numerically from the 'reptation–reaction model' as defined above. These yield direct information on the parameter $\bar{\zeta} \equiv \tau_b/\tau$. For values less than 0.1 the Cole–Cole plot is semicircular, with strong departures for values of order unity. Experimentally, measuring $\tau$ and the shape of the $G^*(\omega)$ spectrum allows $\tau_b$ to be estimated. For example in aqueous CTAB/KBr (0.3 M /0.25 M), $\tau = 95$ ms and the spectrum suggests $\bar{\zeta} = 1.2$. Thus $\tau_b$ is estimated as 115 ms, in good agreement with an independent estimate $\tau_b = 110 \pm 40$ ms from the $T$-jump [9].

Further corrections to the Maxwell spectrum arise at high frequencies. These can be analysed in terms of 'breathing' and 'Rouse modes' which involve the dynamics of a chain on time-scales too short to be fully described by the tube model. The analysis of Granek (see [17]) predicts a minimum value of the loss modulus, obeying (in the crudest approach) $G''_{min}/G_0 \simeq L_e/\bar{L}$. This can be used to get an absolute estimate of the chain length $\bar{L}$ from viscoelastic data. The value of $\bar{L}$ found in this way should show an increasing trend with concentration. This trend is seen, for example, in the system CTAC/NaSal/NaCl [18] with a fixed CTAC/NaSal ratio. At 0.1 M NaCl, $\bar{L}$ is in the range 0.5–1 $\mu$m and increasing with $\phi$. However, at higher salinity (NaCl = 0.25 M) a decreasing trend is seen instead. Various data on other systems suggest that this scenario is fairly common in systems at high salt levels (see e.g. [5]).

It is expected that salt, which suppresses end-caps, should also favour crosslinks and these data have been taken of evidence of branching. The impact of reversible crosslinks on the reptation–reaction model has been examined by Lequeux [19]. He considered 'unsaturated' networks (with relatively few crosslinks) for which a section of chain between crosslinks can still be considered as confined to a tube. Relaxation again requires the section of chain to break, at a point near enough to a given tube segment that the new end can pass

through it before reacting with something else. Lequeux showed that the main effect of crosslinking was through the curvilinear diffusion constant $D_c$ for a chain end. Remarkably, this is enhanced, rather than reduced, by the presence of reversible links: $D_c^{eff} \sim 1/\bar{L}_s$, where $\bar{L}_s \leqslant L$ is the mean strand length between crosslinks. To incorporate Lequeux's result, we need only make the replacement $\bar{L} \to \bar{L}_s$ in our previous discussion. The latter is likely to be a decreasing function of $\phi$ at a fixed salt level, which would explain, in broad terms, the anomalous data on CTAC at high salinity mentioned above.

The recent work of O'Shaughnessy and Yu [13] shows that, like branching, the breakdown of mean-field theory can lead to significant alterations to the basic picture. These authors argued that correlated reactions occur, in reversible-scission systems, when $\tau_b$ (as calculated within mean-field theory) is less than or comparable to $\tau_h$, the mean time taken to diffuse a distance $h$ which is the mean separation between chain ends in the system. For $\tau_b \leqslant \tau_h$, ends repeatedly recombine with their previous partners until a fully effective, uncorrelated break occurs on the time-scale $\tau_h$. Accordingly, $\tau_h$ takes over as the effective breaking time of the system. Note that this mechanism applies only to reversible scission: similar corrections are not expected for the other reaction schemes. The correlated reaction scenario can lead, under some conditions, to a relaxation spectrum which is qualitatively different from that based on mean-field kinetics [13].

## 5. Non-linear viscoelasticity

The linear response theory outlined above is restricted to the limit of small deformations. For general flows, we seek a *constitutive equation* or functional relationship $\sigma_{\alpha\beta}(t) = f\left[K_{\alpha\beta}(t' < t)\right]$, where $K_{\alpha\beta} = \nabla_\alpha u_\beta$ is the velocity gradient or rate-of-deformation tensor. The deformation of a vector due to flow between times $t'$ and $t$ is $r_\alpha(t) = E_{\alpha\beta}(t', t) r_\beta(t')$ where the tensor $E_{\alpha\beta}(t', t)$ will from now on be written as $\boldsymbol{E}_{t't}$. This obeys

$$\boldsymbol{E}_{t't} = \exp\left[\int_{t'}^{t} K_{\alpha\beta}(t'')\ \mathrm{d}t''\right] \tag{12}$$

so $\dot{\boldsymbol{r}} = \boldsymbol{K} \cdot \boldsymbol{r}$.

Consider now the birth and death of tube segments [20]. In the linear region, we have the survival function $\mu(t) = \mathrm{e}^{-t/\tau}$ corresponding to a death rate for tube segments $\mathcal{D} = 1/\tau$. Here the Maxwell limit has been taken. By conservation, this is balanced by a birth rate $\mathcal{B} = 1/\tau$. These rates are modified, however, in non-linear flows. The main effect is called *retraction* [14]. If a random walk is subject to a finite deformation, it increases in length by a factor

$$L'/L = \langle |\boldsymbol{E} \cdot \boldsymbol{u}| \rangle_0 \tag{13}$$

where the subscript 0 denotes the average over an isotropic distribution, $P_0(\boldsymbol{u}) = 1/4\pi$. This stretching effect is compensated by a fast motion in which the chain shrinks back down its tube to restore the original tube length. This causes segments to die at an additional rate [14]

$$v = \frac{1}{L}\frac{\partial L}{\partial t} = \boldsymbol{W}{:}\boldsymbol{K}. \tag{14}$$

The rate $v$ is positive in almost all flows [14], and we assume that applies here. For a non-linear flow, we may approximate $\mathcal{B}$ and $\mathcal{D}$ by

$$\mathcal{B} = 1/\tau \tag{15}$$

$$\mathcal{D} = 1/\tau + v(t) \tag{16}$$

To get a constitutive equation we must find the contribution to the second-moment matrix $\boldsymbol{W}$, at the present time ($t$) due to a segment created earlier, at time $t'$. Such a segment was created isotropically (with probability distribution $P_0(\boldsymbol{u})$) but has been deformed by the flow. Its new length is $|\boldsymbol{E}_{t't} \cdot \boldsymbol{u}|$ and its unit tangent is

$$\boldsymbol{u}' = \frac{\boldsymbol{E}_{t't} \cdot \boldsymbol{u}}{|\boldsymbol{E}_{t't} \cdot \boldsymbol{u}|}. \tag{17}$$

The mean contribution to $\boldsymbol{W}$ from this portion of tube, if it survives, is [20]

$$\hat{\boldsymbol{Q}}_{t't} = \left\langle \frac{\boldsymbol{E}_{t't} \cdot \boldsymbol{u}\ \boldsymbol{E}_{t't} \cdot \boldsymbol{u}}{|\boldsymbol{E}_{t't} \cdot \boldsymbol{u}|} \right\rangle_0 . \tag{18}$$

To calculate the stress at time $t$, we now need only compute $\boldsymbol{W}(t)$ as the sum over contributions from segments born earlier:

$$\boldsymbol{W}(t) = \int_{-\infty}^{t} \mathcal{B}(t')\ \exp\left[ -\int_{t'}^{t} \mathcal{D}(t'')\ \mathrm{d}t'' \right] \hat{\boldsymbol{Q}}_{t't}\ \mathrm{d}t' \tag{19}$$

where the exponential factor is the survival probability between times $t'$ and $t$.

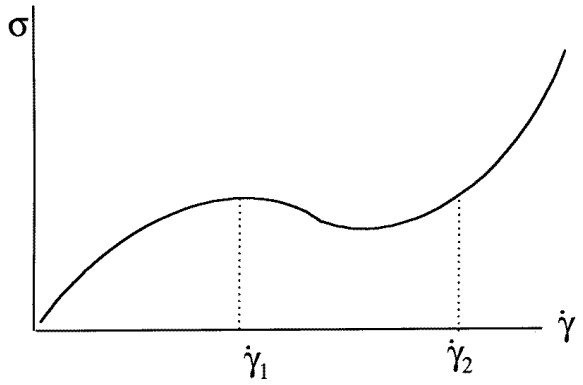


**Figure 1.** A schematic diagram of the curve of shear stress versus strain rate in steady shear flow for an entangled micellar system.

Bearing in mind the relation between the (polymeric) stress $\sigma_{\alpha\beta}$ and $W_{\alpha\beta}$ given previously, this completes the constitutive equation we seek. This can be solved in simple flows, such as steady shear at strain rate $\dot{\gamma}$ [21]. For the polymeric shear stress $\sigma_{xy}^{pol}(\dot{\gamma})$ one finds a curve which shows a maximum shear stress, $\sigma_{max}^{pol} = 0.67G_0$, at shear rate $\dot{\gamma}_1 = 2.6/\tau$. At higher strain rates, the shear stress is a decreasing function of flow rate which corresponds to an unstable flow. The situation is saved (presumably) by a return to increasing stresses at very high flow rates; such an upturn is inevitable, if only from the contribution $\sigma_{\alpha\beta}^{sol}$ of the (Newtonian) solvent which we have been ignoring. We denote by $\dot{\gamma}_2$ the shear rate at which $\sigma_{xy}$ again equals $\sigma_{max}$; for faster flows than this, stable behaviour is recovered. The full stress versus strain rate curve, therefore, should have a local maximum at some flow rate $\dot{\gamma}_1$, followed by a minimum, and then rise again past the original maximum when $\dot{\gamma} = \dot{\gamma}_2$ (figure 1). The actual behaviour of systems whose flow curve looks like this remains a classical and largely unresolved area of non-Newtonian fluid mechanics [22].

Indeed, for $\dot{\gamma}_1 < \dot{\gamma} < \dot{\gamma}_2$, what happens in detail may depend on the precise mechanical specification of the instrument. Typically a cone-and-plate rheometer is used, for which we

might postulate [21, 23] that the observed shear stress obeys $\sigma \equiv \sigma_{xy} = \sigma_{max}$ throughout this region. This is in excellent quantitative agreement with measurements of Rehage and Hoffmann on CPyCl/NaSal (100 mM/60 mM) [15]. The prediction of a constant shear stress arises if one assumes a 'shear-banding instability' where the system coexists between the upper and lower shear rates in bands whose relative volume fractions are chosen to match the imposed macroscopic shear rate $\dot{\gamma}$. There is, however, an additional assumption involved: that of 'top-jumping' whereby one of the participating bands has a polymeric stress $\sigma_{max}$.

Although it seems consistent with the data of reference [15], the top-jumping scenario is far from obvious. On the contrary [24] a recent numerical solution of the constitutive equations in a parallel-plate geometry suggests instead that on increasing the shear rate, the stress should rise to the maximum value $\sigma_{max}$ but then, as the rate is increased further, drop down onto a lower plateau and remain constant. (Similar predictions are obtained for some simplified constitutive models which mimic the non-monotonic flow curve predicted for micelles [24].) Such behaviour has recently been seen in some experiments when controlled-strain-rate rather than controlled-stress machinery is used [25]. It is quite possible that the original observation of an extended stress plateau at $\sigma = \sigma_{max}$, under controlled-stress conditions, is a result of very slow transients. In other words, the data measured along this plateau do not truly correspond to steady-state conditions.

Further careful studies with different rheometric protocols and flow histories are now under way, and the preliminary results [26] strongly suggest that the plateau previously observed at $\sigma = \sigma_{max}$ is indeed not the true steady-state behaviour.

## 6. Outlook

The ultimate resolution of these issues will probably require more sophisticated experimental probes to determine directly (rather than by its impact on the observed stresses) whether a macroscopic flow is homogeneous or not. One promising direction is the introduction of the birefringence microscope [27] which has been used to study an entangled micellar system for which shear banding is expected (although in this case the high-shear branch, $\dot{\gamma}_2$, may correspond to a metastable nematic mesophase). Using this technique, fairly clear evidence for shear banding was found, albeit in a Couette geometry (a bright band is observed close to the inner cylinder of the Couette). Actually in the materials used for this study [28], there is a clear evolution of the observed stress plateau, with temperature and/or concentration, from values near the theoretical (top-jumping) prediction, $\sigma_{max} = 0.67G_0$, to substantially smaller values.

Another potentially vital probe is the direct measurement of flow profiles using NMR imaging [25]. So far this has been used mainly in pipe flow geometries, where, theoretically, there are additional hysteretic features associated with the spurt effect [29], because the shear stress is not constant across the width of the pipe. These features additionally complicate the interpretation of the data which at present cannot be said to support the shear-banding scenario in any definite way [25]. However, there is certainly strong evidence of complex and interesting behaviour at stresses larger than $G_0$. An interesting alternative to shear banding, partly suggested by the NMR studies, is that of wall slip, in which very thin layers of highly deformed material lubricate the walls of the rheometer. The difference from the banding scenario is that these layers must, by definition, be directly altered in their properties by the presence of the wall. When the flow curve is non-monotonic, as predicted for entangled micelles, it is possible that the *constitutive* instability ($\mathrm{d}\sigma/\mathrm{d}\dot{\gamma} < 0$) is the trigger that makes wall slip occur.

In the discussion so far we have tacitly assumed that the 'upturn' in the steady-shear curve does indeed arise from the Newtonian solvent contribution. In fact, at least for the system studied in [15], this is probably untrue, as is evident from the fact that an extremely large, and steadily rising, first normal-stress difference is measured throughout the postulated shear-banding regime (where $\sigma(\dot{\gamma})$ is apparently constant). This does not arise directly in tube models but is predicted by some extensions of them. However, although the simplest such extended model seems to give a good account of the normal-stress data [21, 23], efforts to systematically improve it have tended to decrease the agreement [30]. This area remains open for future experimental and theoretical work.

## Acknowledgments

I wish to thank the many colleagues and collaborators who have made research on this topic over the past decade a stimulating and enjoyable pursuit. I would also especially like to thank Professor S F Edwards and Professor F Y L Pincus for initiating my interest in polymer dynamics and in giant micelles, respectively.

## References

[1] Cates M E 1993 *Phil. Trans. R. Soc.* A **344** 339
[2] Israelachvili J N, Mitchell D and Ninham B 1976 *J. Chem. Soc. Faraday Trans.* II **72** 1525
[3] Cates M E and Candau S J 1990 *J. Phys.: Condens. Matter* **2** 6869
[4] Cates M E 1994 *Structure and Flow in Surfactant Solutions (Symposium Series 578)* ed C A Herb and R K Prud'homme (Washington, DC: ACS Books)
[5] Lequeux F and Candau S J 1994 *Structure and Flow in Surfactant Solutions (Symposium Series 578)* ed C A Herb and R K Prud'homme (Washington, DC: ACS Books)
[6] Hoffmann H 1994 *Structure and Flow in Surfactant Solutions (Symposium Series 578)* ed C A Herb and R K Prud'homme (Washington, DC: ACS Books)
[7] de Gennes P G 1979 *Scaling Concepts in Polymer Physics* (Ithaca, NY: Cornell University Press)
[8] Cates M E 1988 *J. Physique* **49** 1593
[9] Candau S J, Merrikhi F, Waton G and Lemarechal P 1990 *J. Physique* **51** 977
[10] Turner M S and Cates M E 1990 *J. Physique* **51** 307
[11] Turner M S and Cates M E 1991 *Langmuir* **7** 1590
[12] Turner M S and Cates M E 1992 *J. Physique* II **2** 453
Turner M S, Marques C M and Cates M E 1993 *Langmuir* **9** 695
[13] O'Shaughnessy B and Yu J 1995 *Phys. Rev. Lett.* **744** 4329
[14] Doi M and Edwards S F 1986 *The Theory of Polymer Dynamics* (Oxford: Clarendon)
[15] Rehage H and Hoffmann H 1991 *Mol. Phys.* **74** 933; 1988 *J. Phys. Chem.* **92** 4712
[16] Cates M E 1987 *Macromolecules* **20** 2289
[17] Granek R and Cates M E 1992 *J. Chem. Phys.* **96** 4758
and for a recent improvement see
Granek R 1995 *Macromolecules* **28** 5370
[18] Kern F, Zana R and Candau S J 1991 *Langmuir* **7** 1344
[19] Lequeux F 1992 *Europhys. Lett.* **19** 675
[20] Cates M E 1990 *J. Phys. Chem.* **94** 371
[21] Spenley N A, Cates M E and McLeish T C B 1993 *Phys. Rev. Lett.* **71** 939
[22] Vinogradov G V 1973 *Rheol. Acta* **12** 273 and references therein
[23] Cates M E, McLeish T C B and Marrucci G 1993 *Europhys. Lett.* **21** 451
[24] Spenley N A, Yuan X-F and Cates M E 1996 *J. Physique* II **6** 375
[25] Callaghan P T, Cates M E, Rofe C J and Smeulders J B A F 1996 *J. Physique* II **6** 375
[26] Grand C, Arrault J and Cates M E 1996 to be published
[27] Makhloufi R, Decruppe J P, Ait-Ali A and Cressely R 1995 *Europhys. Lett.* **32** 253
[28] Berret J F, Roux D C, Porte G and Lindner P 1994 *Europhys. Lett.* **25** 521
Berret J F, Roux D C and Porte G 1994 *J. Physique* II **4** 1261

and see also
Schmitt V, Lequeux F, Pousse A and Roux D 1994 *Langmuir* **10** 955
[29] McLeish T C B and Ball R C 1986 *J. Polym. Sci., Polym. Phys. Edn* **24** 1735
McLeish T C B 1987 *J. Polym. Sci., Polym. Phys. Edn* **25** 2253 and references therein
[30] Spenley N A and Cates M E 1994 *Macromolecules* **27** 3850